HHS Public Access

Author manuscript

Environ Sci Pollut Res Int. Author manuscript; available in PMC 2017 December 01.

Published in final edited form as:

Environ Sci Pollut Res Int. 2017 August ; 24(23): 18798–18816. doi:10.1007/s11356-017-9342-5.

Distribution of potentially toxic elements (PTEs) in tailings, soils, and plants around Gol-E-Gohar iron mine, a case study in Iran

Naghmeh Soltani[1], **Behnam Keshavarzi**[1], **Farid Moore**[1], **Armin Sorooshian**[2,3], and **Mohamad Reza Ahmadi**[4]

[1]Department of Earth Sciences, College of Science, Shiraz University, Shiraz 71454, Iran

[2]Department of Chemical and Environmental Engineering, University of Arizona, Tucson, AZ 85721, USA

[3]Department of Hydrology and Atmospheric Sciences, University of Arizona, Tucson, AZ 85721, USA

[4]Gol-E-Gohar Iron Ore and Steel Research Institute, Gol-E-Gohar Mining & Industrial Co., Sirjan, Iran

Abstract

This study investigated the concentration of potentially toxic elements (PTEs) including Al, As, Cd, Co, Cr, Cu, Fe, Hg, Mn, Mo, Ni, Pb, Sb, V, and Zn in 102 soils (in the Near and Far areas of the mine), 7 tailings, and 60 plant samples (shoots and roots of *Artemisia sieberi* and *Zygophylum* species) collected at the Gol-E-Gohar iron ore mine in Iran. The elemental concentrations in tailings and soil samples (in Near and Far areas) varied between 7.4 and 35.8 mg kg^{-1} for As (with a mean of 25.39 mg kg^{-1} for tailings), 7.9 and 261.5 mg kg^{-1} (mean 189.83 mg kg^{-1} for tailings) for Co, 17.7 and 885.03 mg kg^{-1} (mean 472.77 mg kg^{-1} for tailings) for Cu, 12,500 and 400,000 mg kg^{-1} (mean 120,642.86 mg kg^{-1} for tailings) for Fe, and 28.1 and 278.1 mg kg^{-1} (mean 150.29 mg kg^{-1} for tailings) for Ni. A number of physicochemical parameters and pollution index for soils were determined around the mine. Sequential extractions of tailings and soil samples indicated that Fe, Cr, and Co were the least mobile and that Mn, Zn, Cu, and As were potentially available for plants uptake. Similar to soil, the concentration of Al, As, Co, Cr, Cu, Fe, Mn, Mo, Ni, and Zn in plant samples decreased with the distance from the mining/processing areas. Data on plants showed that metal concentrations in shoots usually exceeded those in roots and varied significantly between the two investigated species (*Artemisia sieberi* > Z*ygophylum*). All the reported results suggest that the soil and plants near the iron ore mine are contaminated with PTEs and that they can be potentially dispersed in the environment via aerosol transport and deposition.

Keywords

Potentially toxic elements; Mining; Soil pollution; Plant pollution; Sequential extractions

Electronic supplementary material The online version of this article (doi:10.1007/s11356-017-9342-5) contains supplementary material, which is available to authorized users.

Introduction

In areas with mining and mineral processing of metal ores, pollution by potentially toxic elements (PTEs) (Bini and Bech 2014) is a significant issue owing to their transport to soils, biota, and water streams (Keshavarzi et al. 2012; Li et al. 2014; Soltani et al. 2014; Ma et al. 2016). These elements in soils are non-biodegradable and extremely persistent in the environment (Boularbah et al. 2006; Liu et al. 2016), as they accumulate in soils, plants, and water streams leading to health risks for living beings (Clemente et al. 2007; Ji et al. 2013; Luo et al. 2014). Waste tailings in particular are of concern, as they are often left without proper management and are characterized by high potential emissions and high contaminant concentrations (Rodríguez et al. 2009; Rashed 2010; Csavina et al. 2012).

Studies focused on soil contamination near mines often do not consider downstream impacts on plants. Aside from inhalation of wind-blown soil particles, soil-to-plant transfer of trace metals is a pathway of human exposure to soil contamination (Cui et al. 2004; Chojnacka et al. 2005; Rattan et al. 2005). The accumulation of PTEs in plants also suppresses their production (Ryser and Sauder 2006), and the overall growth and crop yield (Athar and Ahmad 2002). The nature of metal transfer from soils to plants, which occurs via roots and shoots (e.g., Bi et al. 2009), depends on plant species and metal type (Alloway 1995). To examine the fate of PTEs in a mining environment, such as the transfer from soils to plants, it is important to characterize the properties of soils and plants. For example, after accumulation of metallic elements in soil, several factors may influence the transfer of PTEs from the solid to the liquid soil phase, causing differences in the availability and toxicity of elements such as Cd, Cu, Mn, or Zn (Moreno-Jiménez et al. 2009). Such factors include total concentration of metals, specific geochemical form, and chemical speciation of metals, pH, electrical conductivity (EC), and soil organic matter (SOM) (Nyamangara 1998; Monterroso et al. 2014). Of importance in the uptake of metals by biota is the quantification of the labile and bioavailable fraction of pollutants (Filgueiras et al. 2002b; Pueyo et al. 2008; Anju and Banerjee 2011; Anjos et al. 2012), which is the fraction available to plants and soil microorganisms.

Sequential extraction procedures (SEPs) are operationally defined methodologies that are widely applied for obtaining quantitative information about both the distribution of PTEs among defined geochemical fractions and their mobility in sediments, soils, and waste materials (Guevara-Riba et al. 2004; Delgado et al. 2011). The mobility, bioavailability, and eco-toxicity of metal/metalloids depend more on their chemical speciation rather than on their total content (Zhu et al. 2014). A number of sequential extraction methods are used at present, and they may differ according to the type of reagent used, the experimental conditions applied, and the number of steps involved (e.g., Tessier et al. 1979; Gibson and Farmer 1986; Dold 2003). One of the most common methods is the Bureau of Reference (BCR) sequential extraction scheme, a simple procedure that has been thoroughly tested by interlaboratory trials (Cappuyns et al. 2007), which harmonize the various SEPs used for geomaterials (sediments, soil, and dust) analysis and which was proposed by the European Community BCR in 1992 (Uren 1992). A modified BCR sequential extraction procedure has been proposed by a group of expert laboratories within the framework of the Standards, Measurements, and Testing (SM&T) Programme of the European Commission to evaluate

the potential mobility and the possible transfer of PTEs from contaminated materials to the surrounding environment (Ariza et al. 2000; Davidson et al. 2006; Rodríguez et al. 2009).

The goal of this study is to report a chemical characterization of soils, tailings, and plant matter from the Gol-E-Gohar (GEG) iron mine in Iran. This work builds on previous studies focused on soil and plant contamination at other mines in the region (Rastmanesh et al. 2010; Keshavarzi et al. 2012; Moore et al. 2016). Mining at GEG began in 1993 with waste/tailings deposits dumped openly in the area surrounding the mine and leaving a legacy of waste rock piles, spoil heaps, and tailing ponds that caused a serious environmental damage. In addition, as a result of the scarcity of water in the region, a major concern is wind-blown dust, as has been documented at mines in other arid regions such as the southwestern USA (Sorooshian et al. 2012; Prabhakar et al. 2014). The objectives of the field measurements include the following: (i) determine the total concentration of selected PTEs (Al, As, Cd, Co, Cr, Cu, Fe, Hg, Mn, Mo, Ni, Pb, Sb, V, and Zn) in soils, tailings, and plants collected around mining and processing areas; and (ii) understand the phase partitioning behavior of selected metals and the ability of selected native plants to accumulate metals from contaminated soils.

Materials and methods

Description of the study area

The GEG mine is located in Southern Iran, in the Kerman Province, approximately 55 km southwest of Sirjan (29.1° N, 55.3° E, 1750 m ASL) (Fig. 1 and S1 (Online Resource)). The facility consists of six separate ore bodies spread over 40 km^2, a primary crusher (PC), a tail bin (TB), numerous tailing piles, a polycom plant (PLY), a hematite recovery plant (HRP), an iron ore concentration plant (ICP), and an iron ore pelletizing plant (IPP). This facility is one of the largest iron ore producers in the region with a total ore reserve of approximately 1135 million tons at a grade of about 57.2% Fe, 0.16% P, and 1.86% S (Monjezi et al. 2009; Nabatian et al. 2015; Hosseini and Asghari 2016).

The Gol-E-Gohar mining and industrial company is capable of producing 14.8 million tons of iron ore concentrate and pellets each year. It employs approximately 3000 workers. Iron is extracted from the low-grade iron ore (mainly magnetite and hematite) by a long process of mining, crushing, separating, concentrating, mixing, pelletizing, and finally shipping for the blast furnace. Briefly, the crude iron ore is mined by detonation with a blasting agent, followed by delivery to large gyrator crushers where chunks as large as 1.5 m are reduced to 200 mm or less. The crushed material is transferred by belt to the concentrator building for grinding, separating, and concentrating. In the ICP plant, the ore is fed into semi-autogenous grinding (SAG) mills, where the ore is reduced to 2 cm or less, then is delivered to a dry magnetic separator, which begins the process of separating the iron from the non-iron material. The material continues to be finely ground in secondary ball mills (125–150 μm), then is moved to hydroseparators, where silica is floated off the top. Thus, the ore is “concentrated” by removing the waste materials. The product is then ready for mixing with the binding agent. In the IPP, a small amount of bentonite, limestone, NaOH, water, and iron concentrated sludge are used to help the iron ore concentrate to stick together when rolled into pellets. Iron ore concentrate is formed into soft pellets through a series of balling drums.

Pellets are screened to meet the size specification (<5 mm). The soft pellets, correctly sized, are delivered to the traveling grate furnace for further drying and preheating at 1200–1500 °C, then discharged into the revolving cooler. Pellets that meet the necessary standards are conveyed to the pellet stockpile. They are shipped to blast furnaces and steel mills, where they are turned into finished steel.

In terms of the geological backdrop of the study site, Paleozoic metamorphic rocks are found in this area, in addition to Mesozoic and Cenozoic sedimentary rocks and Quaternary alluvial materials (Mücke and Younessi 1994; Nabatian et al. 2015). The Mesozoic sediments were deposited along a passive continental margin (Stocklin 1968; Berberian and King 1981; Alavi 2004) and subsequently large-scale Mesozoic plutons ranging from gabbro to granite, emplaced in about 160 ± 10 Ma by the K-Ar methods (Sheikholeslami et al. 2008). The ore bodies show a strong deformation in parallel to the regional west-northwest structural trend. The regional lithologies at GEG record a clockwise metamorphic path subsequent to thrust deformation events during at least three main deformation phases D_1, D_2, and D_3. Based on zircon sensitive high-resolution ion microprobe (SHRIMP) U-Pb and monazite chemical Th-U-total Pb isochron methods (CHIME), a regional metamorphic event occurred between 187 ± 2.6 Ma and 180 ± 21 Ma, respectively. The result of this deformation is a composite foliation between massive magnetite and dolomitic marble that occurred along of a wide ductile shear zone. The D_2 deformation is associated with overthrusting of the old units (e.g., ultramaficmafic rocks) onto the GEG metacarbonate unit and the development of a mylonitic foliation in the various rocks units. D_3 represents an event leading to the development of kink bands, localized shear zones, and slickensides along the thrust sheet of GEG area (Sheikholeslami et al. 2008).

The ore bodies are hosted by a Paleozoic metamorphic sequence of gneisses, quartz biotite schists, calc-schists, quartzites, amphibolites, marble, and dolomitic marble (Monjezi et al. 2009; Nabatian et al. 2015). In the ore deposit, magnetite, pyrite, pyrrhotite, chalcopyrite, pentlandite, sphalerite, and minor apatite are the main ore minerals (Nabatian et al. 2015). A range of sedimentary, volcanosedimentry, and metasomatic processes, as well as magmatism during intracontinental rifting activity have been proposed for the origin of the mine (Mücke and Golestaneh 1982; Heydari 2008). The GEG iron ore is classified as iron oxide copper gold (IOCG) deposit (Williams et al. 2005). The characteristics of the Fe-rich hosts as products of replacement, the distinctive geochemical signatures, alteration styles, and geo-chronological data all point to an epigenetic hydrothermal origin and classification as an IOCG deposit in the GEG area (Williams et al. 2005).

The surroundings of the study site are desert areas with low anthropogenic influence. There are six communities of nomad owning great cattle and sheep herds who come to the area and camp in warm seasons (summer and spring). Figure 1 illustrates the possible position of these six nomads around the studied area. There are sporadic shrubs and steppes around the alluvial plain surrounding the mine. The lack of vegetative covering on the mine tailings and the tailings pile slopes cause instability of the material and allows wind and rain erosion to occur. Minor agricultural activities are to the west of the mine.

The study area is characterized by an arid climate receiving a mean annual precipitation of 134 mm based on data between 2010 and 2014 from the Meteorological Organization of Iran (I.R. of Iran Meteorological organization, IRIMO, Sirjan Synoptic weather station). The dry season lasts from May to October and is characterized by low precipitation. The mean annual temperature is 18.02 °C with the highest being 40.32 °C in July and the lowest being −9.54 °C in December. The prevalent winds in the study region are south-easterly with a mean annual speed of 3 m s^{-1} and maximum speeds in August. As a result of hot and dry climate in the region and very low concentrations of SOM, soils exhibit a poorly developed layering.

Soil and tailing samples

About 109 surface soil and tailing samples were collected during two-field campaign intensive periods in the months of April 2013 and December 2014. The sampling sites in Fig. 1 are classified in three groups according to location and degree of contamination. The first group was taken close to the open pits and industrial plants with strong anthropogenic influences from iron ore mining and mineral processing (Near). The second group is located far from the industrial plants and open pits, at a development site for mining and facilities (Far). The third group consists of samples taken from tailing piles near the mine (Tailings). Figure S1 (Online Resource) shows a close-up of the Tailings and Near areas. Nine soil samples were also collected at 30–40 cm depth in the Far areas from locations with no mining and processing activities, which can be considered as unaffected soils or, at least, minimally affected by human activities. These soils were used as reference soil or control soil samples to estimate the PTE geochemical baseline concentrations (GBCs) and to calculate the geoaccumulation index (I_{geo}).

Each soil sample (nearly 1 kg, 29 samples from the Near and 64 sample from the Far area) consisted of a composite sample, prepared by mixing four subsamples taken at 0–20 cm on the edges and in the center of a 1-m^2 area, after removal of plant remains and humus layer according to Qin et al. (2014).

Tailing samples ($N = 7$) were collected in tailing piles from waste materials generated during dry magnetic separation process using a stainless steel hand trowel. All soil and tailing samples were thoroughly mixed to ensure that the sample was representative of the whole sampled material and then transferred to the medical geology laboratory at Shiraz University. Samples were dried and then sieved through a 2-mm screen, to remove coarse materials. The fine soil fraction (<2 mm) was used for determining the physicochemical properties of soils (Alvarez et al. 2003; Basta and McGowen 2004; Abreu et al. 2012; Bech et al. 2012a; Bes et al. 2014). The 2-mm fraction of the soil samples was stored in polyethylene bags in dark and dry conditions at room temperature for subsequent analysis. In addition to the surface soil and tailing samples, 10 “fallout dust” samples were collected by brush swabbing across a clean non-porous collection surface with a 100-cm^2 surface area, which was placed at 1 m above ground level and washed with distilled water before sampling. These samples were collected inside ICP, PC, IPP, HRP, PLY, and near TB and the research and development center (in the Near area), and then analyzed using the same methods adopted for soil analysis.

A number of tests were carried out to characterize the sub-2 mm soil properties: (i) Soil grain size was determined using the hydrometer method (Gee et al. 1986). (ii) Soil mineralogy ($N = 15$) was assessed using semi quantitative X-ray diffraction analysis with PROFEX software (version 3.10.2; Döbelin and Kleeberg, Bettlach, Switzerland) (Dobran and Zagury 2006) and the Rietveld refinement kernel BGMN (version 4.2.22, Netherlands Energy Research Foundation ECN, Rietveld, Petten, The Netherlands). By using this method, clay mineral, mica, and chlorite structures are relatively easily identified (Meunier 2005; Asadi et al. 2013). X-ray diffraction patterns were collected using MPD 3000 multipurpose XR diffractometer (Italy, GNR Company). (iii) Acidity of the soil samples was determined by placing 50 g of sample in 50 ml distilled water followed by agitation for 10 min. The solution was left undisturbed for 30 min with occasional shaking before measuring the pH. A combined glass electrode connected to a pH-meter (Eutech instrument, Waterproof CyberScan PCD 650, Singapore) was used for pH measurements. (iv) EC was measured in 1:5 water extracts (w:v) with a conductivity-meter (Eutech instrument, Waterproof CyberScan PCD 650, Singapore) after 1 h of mechanical agitation, centrifugation, and filtration. (v) SOM content was determined by oxidation with potassium dichromate and colorimetric determination (Nelson et al. 1996). (vi) Cation exchange capacity (CEC) was measured using ammonium acetate method after washing with alcohol (Kahr and Madsen 1995). (vii) Total concentrations of PTEs were determined by using inductively coupled plasma mass spectrometry (ICP/MS; model PerkinElmer EIAN 9000) at Acme Analytical Laboratories (Canada). Approximately 0.25 g of prepared samples (<63 μm) were heated in a concentrated HF-HNO_3-$HClO_4$ mixture and taken to dryness. The residue was dissolved in mixture of three volumes of HCl (37%) and one volume of HNO_3 (67%), and the digested solution (after dilution in distilled water up to 25 ml) was subsequently analyzed by ICP/MS. (viii) The modified BCR sequential extraction scheme was used for metal fractionation analysis (Yan et al. 2010). Trace element concentration in each fraction was determined by inductively coupled plasma-optical emission spectrometry (ICP-OES) (Agilent model 735, United States) at Zarazma Mineral Studies Company (Iran) in order to identify how the elements were distributed among the soil components. The detection limits for ICP-OES are as follows: 0.05 mg l^{-1} for As, Co, Cr, Cu, Ni, and Zn and 0.1 mg $l^{-}{}_1$ for Fe and Mn.

QA/QC included the analysis of reagent blanks, analytical duplicates, and certified reference material (CRM) like multi-element STD OREAS45e and OREAS45c and an internal standard STD DS9 for soil and STD CDV-1 and STD V16 for plant. The recovery rates for the considered metals in the OREAS were given on the standard certificate between 95 and 110%.

Plant samples

Plant samples were simultaneously collected with the soil samples at the same sites in Near and Far areas (Fig. 2). No plants were present at the tailings dump. Sixty plant samples were collected from two abundant indigenous plant species (*Artemisia sieberi* and *Zygophylum*) that were common to all the areas where soil samples were collected. These two plants are also important as livestock feed and having been studied in other mines in the region. Plant samples were transferred immediately to the laboratory and carefully rinsed with tap water

followed by distilled water to remove adhering materials and dried in a clean room at 25 °C for 5 days. Roots and shoots were studied separately to obtain information about the species' ability to transfer metals. Dried plant tissues were powdered and repackaged in a plastic bag. The plant samples were examined for total metals concentration using the same method described above for soil samples.

Soil samples calculations

The term GBC is often used to express an expected range of element concentrations in soils; it is not generally a true baseline (BL) and is defined as 95% of the expected range of background concentration (Ramos-Miras et al. 2011). Identification of the GBC of PTEs in the soil is important for assessing soil pollution (Albanese et al. 2007; Galán et al. 2008). Baseline concentrations of PTEs were calculated using the method proposed by Reimann et al. (2005). The median ± 2MAD (median absolute deviation = median_i ($|X_i - \text{median}_j (X_j)|$) is better suited for the estimation of threshold values and the range of background data (Reimann et al. 2005; Tume et al. 2008; Teng et al. 2010) which was used previously (Esmaeili et al. 2014; Rastegari Mehr et al. 2016). ($|X_i - \text{median}_j (X_j)|$) is a measure of absolute difference between the observed value of a variable and the median of the data set. X_i is the observed value of a variable or the data element. $\text{Median}_j (X_j)$ is the median of the data set. The median and MAD are inherently stable against outliers and deviations. In most cases, they give much more realistic values for location and spread (Reimann and Filzmoser 2000). Because of the lognormal distribution of elements in geological materials (e.g., Salminen and Tarvainen 1997; Reimann et al. 2005), it is assumed that the median (value at the 50th percentile of the background data) can serve as the soil geochemical baseline for each element, reflecting natural processes unaffected or diffusely affected by human activities (Galán et al. 2008). Prior to calculation, the Kolmogorov–Smirnov (K–S) test was conducted to check the concentration distributions of PTEs. The results of the K–S test indicate that PTE distributions are nearly normal.

The I_{geo}, originally defined by Müller (1969), has been used to evaluate the pollution level of PTEs in soils (Loska et al. 2004), sediments (Shafie et al. 2013), and tailings (Levei et al. 2013). It can be calculated using:

$$I_{\text{geo}} = log_2 \left(C_n / 1.5\, B_n \right) \quad (1)$$

where C_n is the measured concentration of the metal ions in soil, B_n is the geochemical background value (local baseline) of the corresponding metal, and the coefficient 1.5 is used to detect very small anthropogenic influences (Müller 1969). According to Müller (1969), the corresponding relationships between I_{geo} and the pollution level are as follows: unpolluted ($I_{geo} \leq 0$), unpolluted to moderately polluted ($0 < I_{geo} \leq 1$), moderately polluted ($1 < I_{geo} \leq 2$), moderately to heavily polluted ($2 < I_{geo} \leq 3$), heavily polluted ($3 < I_{geo} \leq 4$), heavily to extremely polluted ($4 < I_{geo} \leq 5$), or extremely polluted ($I_{geo} > 5$).

Plant sample calculations

Plant bioaccumulation factors (BAF) were determined by using the following equations:

$$BAF_{shoot}=C_{[\mathrm{PTE}\ in\ shoot]}/C_{[\mathrm{PTE}\ in\ soil]} \quad (2)$$

$$BAF_{root}=C_{[\mathrm{PTE}\ in\ root]}/C_{[\mathrm{PTE}\ in\ soil]} \quad (3)$$

where C_{PTE} represents PTE concentration in either plants (shoot and root) or soil (Ma et al. 2001; Yoon et al. 2006). The translocation factor (TF), the plant capacity to translocate PTEs, was calculated as follows:

$$TF=C_{aerial}/C_{root} \quad (4)$$

which is the ratio of PTEs concentration in the plant shoot (C_{aerial}) to that in the root (C_{root}). This coefficient is used to evaluate the ability of plants to transfer PTEs from the roots to their aerial parts (Sun et al. 2008; Sun et al. 2009).

Statistical analysis

The experimental data were treated statistically using SPSS software (Version 19.0 for Windows). In order to avoid problems associated with normal/non-normal distribution, the K–S and Shapiro-Wilk tests were used for identification of data distribution. Most results exhibited a non-normal distribution and local baseline samples showed a normal distribution. Spearman's correlation coefficient analysis and principal component analysis (PCA) were used to determine the relationship among PTEs in soils and their possible sources. The Kruskal-Wallis non-parametric tests were conducted to verify the significance of possible differences between PTE concentrations in soil and plant samples collected from different sites, with significance being established at the 5% level (i.e., $p < 0.05$) (Table S1 and S2 (Online Resource)). The Mann-Whitney U test was employed to examine the statistical significance of the differences in the mean concentrations of PTEs among different soil samples in Near and Far areas.

Results and discussion

Soils

Physicochemical properties—The physicochemical characteristics of the studied soils are categorized into three areas (Near, Far, and Tailings) where representative samples were collected at GEG (Table 1). The soils are characterized by neutral to alkaline pH ranging from 6.87 to 8.63. The EC values ranged between 235.1 and 8903 μS cm^{-1}. The CEC values ranged from 1.8 to 20 meq 100 g^{-1}. The total SOM contribution to total soil mass ranged from 0.07 to 1.52% (on mass basis), which is expectedly low as with soils in other desert regions (Pascual et al. 1997); therefore, SOM is expected to have a limited importance in governing trace element behavior in soils. The role of SOM in solubilization, transport, and adsorption/coprecipitation processes of PTMs is reported by several authors (Halbach et al. 1980; Stevenson 1983; Thanabalasingam and Pickering 1985; Kabata-Pendias 2010).

Mineralogy—To understand the mineralogical nature of the soil at the study site, X-ray diffraction analysis was carried out for 15 representative samples (8 in Near, 6 in Far, 1 in Tailings). The results show that the soil minerals in the bulk soil were very similar in all the samples and consisted mainly of calcite, quartz, talc, albite, muscovite, clinochlore, microcline, magnetite, chlorite, and kaolinite with minor amounts of montmorillonite, pyrite, biotite, ferroactinolite, hematite, dolomite, gypsum, halite, and antigorite (Table S3 (Online Resource)).

Semi-quantitative estimates of the mass percentage contribution of major minerals, reported as a range, are as follows: calcite (6.2–66.2%) > quartz (5.5–38.8%) > talc (12.3–38.4%) > albite (6.6–30.3%) > muscovite (1.8–25.2%) > chlorite (1.7–19.2%) > clinochlore (6.1–17.6%) > microcline (4.4–17.3%) > magnetite (8.5–12.8%) > kaolinite (3.3–9.6%).

Elemental concentrations—Data and statistics on PTE concentrations in tailings, soils, local baseline, and fallout dust are summarized in Table 2. The K–S test indicated that the concentration of all elements in the local baseline were distributed normally, but the concentration profile of all PTEs, except Hg, in Tailings, soil in Near and Far areas, and fallout dust samples, exhibited non-normal distributions (p n0.05). In these samples, the concentrations of all trace and major elements (Al, Fe, and Mn) exhibited relatively high coefficients of variation (CV), suggesting that their inputs into soils in the study area derived from anthropogenic sources. The PTEs with mean and median concentrations exceeding the world soil average (Kabata-Pendias 2010) and local baseline, regardless of location at GEG, included As, Co, Cu, Fe, Mo, and Ni. On the other hand, the higher contents of some elements relative to world soil average such as Al, Cr, and Mn in deeper soil horizons (30–40 cm, used as local baseline samples) are probably due to primary minerals. The highest mean and median concentrations of Al and V were found in the Near category, but when comparing the maximum concentrations, also several other species were the highest in Near samples (As, Cr, Fe, Mo, and Zn). For the Tailings, mean, median, and maximum concentrations of Co, Cu, Mo, and Ni were the highest among all samples. Arsenic and Fe also showed the highest mean and median concentrations in Tailing samples. PTEs such as Al, Cd, Hg, Pb, and Sb exhibited low concentrations and were below the world soil average.

In the Far area, Cr, Mn, and Pb appeared significantly enhanced in concentration. The mean concentrations of Pb in Near and Far areas were 10.8 and 15.07 mg kg^{-1}, respectively, which anyway are lower than their world soil average values (25 mg kg^{-1}). The average concentrations of Mn in Near and Far areas were 544.63 and 643.84 mg kg^{-1}, respectively. The increased concentration of Mn in the Far area may result from the fact that during ore genesis (IOCG mineralization type), Mn, which has normally a high solubility, is transported laterally by hydrothermal fluids and then precipitated further up in the intrusion, or distal to it (Barnes 1997; Pirajno 2009). The Mann-Whitney test showed that there were significant differences between Mn and Pb concentrations in Near and Far areas. Chromium concentration in Near and Far areas did not exhibit significant differences. In the study area, metal/metalloid pollution in soil is derived mostly from natural iron ore mineralization and also atmospheric fallout generating during iron ore processing activities and tailing emission, resulting in elevated potential risks to human health and the local environment.

Elemental concentrations in fallout dust were almost of the same magnitude of those in the Tailings and Near categories (Table 2), thus providing support for contaminants being transported by dust and depositing around the mining facility. The high contents of As, Co, Cu, Fe, Mo, Ni, and V in Tailings and topsoil in the Near area in relation to those detected in the local baseline clearly indicate contamination by fallout dust coming from the ore processing plants and tailings piles. Liénard et al. (2014) concluded that severe contamination of topsoil by Cd, Cu, Pb, and Zn within a 3-km radius circle surrounding stacks of a former Zn-Pb ore treatment plant of the Sclaigneaux calaminary site in Belgium is probably driven by anthropogenic factors, specifically historical industrial activities and subsequent atmospheric deposition. Li et al. (2015) also reported that Pb/Zn smelting and resulting dust fallout have led to significant contamination of the local topsoil by Zn, Pb, Cd, As, Sb, and Hg in a town in Yunnan Province of China. Kříbek et al. (2014) indicated that high amounts of Zn, Pb, Mn, Cu, Cd, As, and Hg in topsoil close to the Pb-Zn Rosh Pinah mine in Namibia are a result of dust blown out from the tailings dam and the ore treatment plant.

Earlier studies have shown that distance from the source and meteorological factors play important roles in exposure to metals and metalloids. PTE concentrations in Near and Far areas showed that contaminant concentrations were highest near the mining and processing plants. For example, a study by Benin et al. (1999) showed that As, Pb, and Cd in roadside dust near Torreón (a nonferrous smelting and refining site in Mexico) decreased with distance and reached background values 1.5–2 km from the smelter. Taylor et al. (2010) determined that elevated concentrations of Cd, Cu, Pb, and Zn in soil around the mining area of Xstrata Mount Isa Mines in Queensland, Australia, were a consequence of mining emissions. Over sufficient time, large amounts of contaminants can be dispersed by wind, water, and anthropogenic activities (along trackways where mined ore are transported) and may result in large variations in concentrations both horizontally across an area and vertically through the soil profile. This consequently may lead to elevated potential risks to human health and the local environment.

Relationship between mineral and elemental composition of soil—Locally, mineralized bedrocks (ores) can contain high elemental concentrations, resulting in geogenic anomalies in soil (Alloway 2012). In mining districts, mineralogy, natural distribution of elements, and chemical composition of soil are strongly controlled by the mineralization type and occurrence of ore and minerals in the region. According to the mineralogical study of GEG iron ore, the most important minerals include magnetite, pyrite, pyrrhotite, chalcopyrite, pentlandite, and sphalerite. Alteration minerals such as actinolite, olivine, hornblende, phlogopite, chlorite, and carbonates are associated with the Fe-oxide minerals (Nabatian et al. 2015). Gol-E-Gohar mine is classified as IOCG type (Williams et al. 2005). The IOCG-related magnetite-rich deposits are generally depleted in Cr and Mn relative to Fe (Kisvarsanyi and Proctor 1967; Frietsch 1978; Hauck 1990) and rich in a few elements like Co and Ni in small amounts, typically in pyrite, pyrrhotite, and locally, discrete Ni and Co sulfides that have been of economic interest (e.g., Mazdab 2001; Monteiro et al. 2008; Pal et al. 2009; Rusk et al. 2010; Slack et al. 2011). Geogenic Co is present in the divalent state (Co^{2+}) and is found primarily associated with ferromagnesian minerals where their

respective divalent radii allow it to substitute readily for Fe(II) and Mg by isomorphous substitution (Goldschmidt 1958; Hooda 2010; Kabata-Pendias 2010). Nickel is generally distributed with other elements, such as Co and Fe (Uren 1992). The ionic properties of Ni allow it to substitute for several alkaline and metallic cations, such as Mg, Al, Fe(II), Fe(III), Mn(II), Mn(III), and Cu, in primary minerals such as magnetite and biotite (Moore and Reynolds 1997; Gonnelli and Renella 2013). Some Fe-bearing phases like magnetite, hematite, and epidote generally contains minor amounts of V, Co, As, and Ni (Barton 2013). In this type of deposit, magnetite compositions can be highly varied (Monteiro et al. 2008; Rusk et al. 2010; Xavier et al. 2012). Iron can occur in primary minerals in the form of crystalline Fe-oxide and ferromagnesium silicates (Krauskopf 1979).

Besides, the most important anthropogenic source of contamination of soils and plant in mineralized area is the dust fallout from mining and processing operations and from dry parts of tailings piles and ponds. Fallout dust can disperse over a wide area and may negatively affect the soil and plant in the area surrounding the facility. Mineralogical studies of particulate matter generated by grinding of iron ore indicated that dominant minerals include magnetite, hematite, kaolinite, talc, tremolite, calcite, albite, pyrite, and actinolite and minor amounts of quartz, hematite, dioptase, biotite, sphalerite, albite, chalcopyrite, nimite, magnesiohornblende, and muscovite (Soltani et al. 2017). The mineralogical study of 15 representative soil samples proved the presence of primary minerals such as crystalline Fe-oxide (magnetite and hematite) and ferromagnesian minerals (biotite, ferroactinolite, chlorite, antigorite, talc, and clinochlor). Therefore, a distinctive and broad suite of minor elements can be released from these minerals.

Index of soil pollution—In this work, the I_{geo} has been applied to assess trace element enrichment and contamination in soils. Table 2 summarizes I_{geo} values in soils and tailings (relative to the local baseline). I_{geo} values, which quantify levels of contamination, are as follows in decreasing order: Cu (3.1 > 0.43 > −0.48), Co (3.2 > 0.36 > −0.51), Fe (1.49 > 0.62 > −0.39), Mo (1.3 > 0.04 > −0.34), As (0.67 > 0.04 > −0.4), and Ni (0.45 > 0.04 > −0.56) in Tailings, Near, and Far areas, respectively. I_{geo} values reaching peak values in the Tailings category included Cu, Co, Fe, Mo, As, and Ni (Table 2). Using the criteria defined by Müller (1969) in “Soil samples calculations” section, only Cu and Co qualify as being “heavily polluted” ($3 < I_{geo} \leq 4$). Iron and molybdenum qualify as “moderately polluted” ($1 < I_{geo} \leq 2$), and As and Ni qualify as “unpolluted to moderately polluted” ($0 < I_{geo} \leq 1$) in Tailing samples. The Near area can be qualified as unpolluted to moderately polluted for the above mentioned elements along with V. Far areas can be classified as “unpolluted” for all the mentioned elements ($I_{geo} \leq 0$). For the rest of the elements, all samples fall in the category “unpolluted” (Table 2). Therefore, the I_{geo} results suggest that several PTEs, especially Cu, Co, Fe, Mo, As, and Ni, in Tailings and partly in Near soil samples are affected by human activities (mining and mineral processing of iron ore).

Source of PTEs contamination in soil—To identify interrelationships and potential sources for the studied PTEs, correlation coefficient analysis and PCA were conducted (Table 3). The correlation coefficients showed that some elements such as As, Cu, Co, Fe, Mo, Ni, and V display strong positive correlations with each other at $p < 0.01$ and negative

correlations with the rest of elements. This may be attributed to differences in their concentrations as well as to their geochemical behavior. With consideration to Table 2, it is clear that the concentration of these elements decreases from Tailings and Near areas to Far areas.

A significant positive correlation was also found between Al, Cd, Cr, Hg, Mn, Pb, Sb, and Zn ($p < 0.01$). These elements are not enriched in iron ore mine in the study region.

The results of PCA for PTEs are also shown in Table 4. Three principal components (PC1, PC2, and PC3) with Eigen values higher than 1 were extracted. The three PCs cumulatively accounted for 69.0% of the total variation within the variables. The first principal component (PC1) mainly included PTEs such as As, Co, Cu, Fe, Mo, Ni, and V. The PTEs in the PC1 were strongly correlated with each other. PC2 explained 16.6% of the total variance and has significant loadings for Al, Cr, Mn, and Sb, which are significantly correlated with each other except for Sb in Table 3: Al-Cr ($r = 0.810$, $p < 0.01$), Al-Mn ($r = 0.498$, $p < 0.01$), and Mn-Cr ($r = 0.613$, $p < 0.01$). PC3 is the weakest, explaining only 9.6% of the total variance and with its highest loading being for Cd, Hg, Pb, and Zn. Zinc and Pb have also similar geochemical characteristics.

The results from the multivariate statistical analysis are consistent with the soil pollution index (I_{geo}) of PTEs in that some elements such as As, Co, Cu, Fe, Mo, Ni, and V originate from the same natural mineralization of iron ore in the region and also from the same anthropogenic sources such as mining and processing activities (facility emissions) and improper disposal of waste and tailings. The range and mean concentrations of Al, Cd, Cr, Hg, Mn, Pb, Sb, and Zn are low (with “unpolluted” I_{geo} degree) providing more support that their distribution probably was not affected by mineralization and anthropogenic activities (mining and processing).

Phase partitioning of metals—A modified BCR sequential chemical extraction was carried out in order to identify the distribution of PTEs (As, Co, Cr, Cu, Fe, Mn, Ni, and Zn) in different geochemical soil fractions for 12 samples (6 in Near, 4 in Far, 2 in Tailings) (Fig. 3, Table S4 (Online Resource)), the mean of which will be reported in the subsequent discussion.

The acid extractable/exchangeable fraction (F1; e.g., carbonates) includes weakly adsorbed metals retained on the solid surface by relatively weak electrostatic interaction (Filgueiras et al. 2002a) and metals that can be released most readily into the environment by ion-exchange processes (Stone and Droppo 1996; Rodríguez et al. 2009). As the most reactive fraction, the acid-soluble fraction should be considered with more attention owing to its higher potential availability to ecosystems. Metals corresponding to the exchangeable fraction usually represent a small portion of the total metal content in soil (Hall et al. 1996; Rauret 1998). Therefore, not surprisingly, the percentage of the metals in F1 of the GEG examined soils was very low and followed this order: Mn > Zn > Cu > As > Ni > Cr > Co > Fe. It is visible from Fig. 3 that in most samples, Mn was present at higher percentages (with an average of 15.34%) in the acid-soluble fractions (the most labile fraction), suggesting that Mn is more mobile and potentially more bioavailable in soil. The relatively higher

percentage of Mn in the weakly bound fraction was probably due to its special affinity for carbonate (Nemati et al. 2009; Qiao et al. 2013; Liu et al. 2015). Soils from the studied area contained variable amounts of carbonate minerals, specially calcite and dolomite (as indicated by XRD analysis). Carbonate can be an important adsorbent for many metals when SOM and Fe–Mn oxides are less abundant in the environment (Stone and Droppo 1996). Unlike Mn, among the elements analyzed, Fe was the least mobile in soil with the lowest percentage (0.04–0.74%) in the acid-soluble fraction. These results indicate that Fe had the strongest association to soil.

The largest percentages of the easily reducible fraction (F2; e.g., amorphous iron/manganese oxides and hydroxides) were observed for Mn, Zn, As, Cu, Ni, and Co: 34.39, 32.29, 29.07, 22.96, 20.51, and 20.00%, respectively (Fig. 3); the lowest were observed for Cr and Fe: 12.35 and 6.68%, respectively. Fe-Mn oxides play an important role in the fixation of metals, especially Zn, As, and Cu. The high affinity of Cu for these oxides was previously suggested by Cerqueira et al. (2011), Vega et al. (2010), and Arenas-Lago et al. (2014). These oxides are well-known “sinks” in the surface environment for PTEs and are thermodynamically unstable under anoxic conditions (Anju and Banerjee 2010). In the present study, Mn and Zn were the PTEs mostly extracted in the first and second steps (about 49.73 and 40.80%, respectively) in all 12 samples.

Iron and Cr in most samples were present at lower percentages (3.6–15.67% and 6.36–20.00% for Fe and Cr, respectively) in F2 fraction reflecting that Fe and Cr were the least mobile in the soils from GEG mine. Iron and Cr are usually found associated with clay minerals such as smectite, montmorillonite, illite, and vermiculite rather than in Fe oxides and hydroxides in soils and sediments (Sposito 1983). In addition, the availability of Fe is related to pH and oxidizing-reducing conditions of soil (Siegel 2005). Iron is immobile in different conditions of pH (oxidizing environment, pH < 4 and pH = 5–8) and Eh (reducing environment) because of its low equilibrium constant ($k_{eq} < 0.1$) (Levinson 1974; Rose et al. 1979). Therefore, it is concluded that Fe and Cr are the least mobile elements in the study area. Chao and Zhou (1983) showed that after certain reaction time, 30–60 min in 0.25 mol l^{-1} hydrox-ylamine hydrochloride ($NH_2OH.HCl$) and 0.25 mol l^{1} HCl at 70°, hydrous iron/manganese oxides and minor crystalline Fe oxides (<1% of the total iron) except for magnetite (ca. 2%) dissolve from soil and sediment. Therefore, Fe in GEG soils is probably present as crystalline Fe oxides like magnetite, which are not extractable in this step.

The highest percentages of metals associated with the oxidizable fraction (F3; e.g., SOM and sulfides) were observed for As (25.90%), Ni (16.00%), Co (14.46%), and Cu (13.81). It has been found that the percentages of all the elements bound to this fraction are in general lower than those associated with the Fe/Mn oxides, thus suggesting a lower contribution of SOM and sulfides to the speciation of these elements. The dissolution of SOM and sulfides under oxidizing conditions can lead to the release of PTEs bound to these components (Filgueiras et al. 2002a). Such changes may occur for example during the oxidation of metal sulfides, specifically in a base-metal mining area rich in sulfide ores (Anju and Banerjee 2010). Since the SOM content of the investigated soils is very low, probably these PTEs could be associated with sulfides rather than to SOM. In fact, previous mineralogical studies

revealed the presence of sulfide minerals, especially pyrite, chalcopyrite, pyrrhotite, pentlandite, and sphalerite in GEG iron ore (Nabatian et al. 2015; Soltani et al. 2017).

The residual (e.g., silicate bound metals) fraction (F4) exhibited high percentages for Fe (88.30%), Cr (74.80%), Co (61.50%), Ni (58.75%), Cu (56.75%), and Zn (53.65%). In this fraction, metals have the strongest associations with the crystalline structures of the minerals and are therefore the most difficult to extract and hardly escape from the restriction of crystal lattice (Tessier et al. 1979; Anju and Banerjee 2010; Liu et al. 2015; Sipos et al. 2016). The high percentage (>50%) of Fe, Cr, Co, Ni, Cu, and Zn in the residual fraction suggests that a large amount of these elements derives from geogenic sources (iron ore mineralization in the area). Tessier et al. (1979) suggested that metal/metalloid concentrations in the residual fraction of soils or sediments may be indicative of background metal levels.

This also suggests that under changing environmental conditions, these metals in soil samples are scarcely bioavailable, as they are considered to be stabilized within the mineral matrix, as it has been previously reported (Li et al. 1995; Maiz et al. 1997; Nemati et al. 2009; Osakwe 2013). Osakwe (2013) demonstrated that the residual fraction containing Fe, Ni, and Cr content (an average of 74.43, 70.11, and 64.47%, respectively) constituted the predominant species of these metals in a soil from southeastern Nigeria contaminated with PTEs as a result of anthropogenic activities such as agriculture, building construction, and urbanization. Arenas-Lago et al. (2014) reported that Cr and Ni are strongly retained in the residual fraction and fixed in soils contaminated by mining activities at the Touro copper mine in Spain, and their mobility is limited. Chai et al. (2015) also reported that Cr and Ni were dominant in the residual fraction in grassland soils from the Baicheng–Songyuan area, China. García-Ordiales et al. (2016) found that Co, Cr, and Ni exhibited high contents in the residual fraction, supporting the hypothesis that these elements are lithogenic and probably associated with stable silicates or sulfide minerals.

Iron is a major element in soil with a median value of 2.1% (Rose et al. 1979). It is present mostly as Fe^{2+} in ferromagnesian silicates or rock forming minerals, including olivine, pyroxene, amphibole and mica (specially biotite), and as Fe^{3+} in iron oxides and hydroxides, as a result of weathering. It has both lithophile and chalcophile properties due to its low electronegativity ($E = 1.8$) (Goldschmidt 1937; Krauskopf 1979), forming several common minerals, including pyrite FeS_2, magnetite Fe_3O_4, hematite Fe_2O_3, and siderite $FeCO_3$ (Zumdahl and DeCoste 2014). Iron is relatively immobile under most environmental conditions and generally has a very low bioavailability in soil (Hooda 2010), mainly due to the very low solubility of iron (III) hydroxide in its various forms. Chromium also was predominantly bound to the residual fraction, which may be linked to the preferential incorpo-rationofCrintothelatticeofsilicatesandprimaryoxidesminerals (Vithanage et al. 2014; Arenas-Lago et al. 2016). Chromium in soil is strongly retained by the solid phases and is generally poorly soluble and not mobile owing to its ionic properties (oxidation state and redox potential) (Alloway 2012). Therefore, the high amount of Fe and Cr in the residual and aqua-regia non-soluble fraction suggests that, in the studied soils, they are primarily associated to silicates and oxides (especially magnetite).

In summary, in most of the cases, the residual fraction of the studied soils contains the highest proportion of PTEs. However, although the highest content of PTEs is in fractions with limited mobility, care must be taken, since the various environmental conditions of the soils may cause their displacement to more mobile fractions, thereby increasing their mobility and availability. The mobility and toxicity of PTEs in soil depend largely on their speciation. Mobility factor (MF) is commonly used to determine element mobility, which is calculated using the species fraction of element by the following equation (Kabala and Singh 2001; Achiba et al. 2010; Kabata-Pendias 2010):

$$MF = \frac{F1}{F1+F2+F3+F4} \times 100 \quad (5)$$

The mean MFs for Mn, Zn, Cu, As, Ni, Cr, Co, and Fe in 12 representative soil and tailing samples were 20.94, 17.16, 8.85, 6.1, 5.87, 4.05, 2.95, and 0.22, respectively (Table S4 (Online Resource)). This indicates that Mn, Zn, Cu, and As are the most likely to be taken up by plants and living organisms. Chromium, Co, and Fe can be regarded as the most stable PTEs due to their low MFs.

Plants

Elemental concentrations—A summary of PTE concentrations in the selected two plant species grown in the vicinity of GEG mine in Near and Far areas (*Artemisia sieberi* and *Zygophylum*) is shown in Table 5. Shoot and root concentrations are reported for *Artemisia sieberi*, while only shoot concentrations are shown for *Zygophylum* due to the difficulty to get root samples. The Kruskal-Wallis statistical test revealed that PTE concentrations exhibited significant differences for all the studied elements except for V (Table S2 (Online Resource)). The mean concentrations of As, Co, Cu, Fe, Ni, and Zn in aerial parts (i.e., shoots) of the *Artemisia sieberi* in the Near category were 1.54, 2.79, 31.7, 6764.29, 7.45, and 64.95 mg kg^{-1}, respectively. Concentrations of these selected elements in the roots of *Artemisia sieberi* were lower (mg kg^{-1}): As (1.12), Co (1.28), Cu (17.8), Fe (3229.09), Ni (5.59), and Zn (21.8). Few elements (Cd, Hg, Sb, and V) exhibited similar values in both shoots and roots. Bech et al. (2012a, b) also showed that plants growing in contaminated soils near the Carolina polymetallic mine in the Peruvian Andes contained higher As, Fe, Mn, Pb, and Zn concentrations in their edible parts as compared to roots. Rashed (2010) reported that plant samples (*Acia raddiena* and *Aerva javanica*) near the tailing sites in Egypt contained higher metal concentrations (Ag, Au, As, Cd, Cu, Co, Cr, Mo, Mn, Ni, Pb, and Zn) than those from other sites far from tailings. Table S5 (Online Resource) shows a comparison of PTE concentrations in the shoots and roots of *Artemisia* species in the study area and other mining districts in Iran and industrial areas of Azerbaijan. Some elements such as Co, Cr, Fe (in roots and shoots), and Ni (in shoots) have a higher concentration, while As, Cd, Mo, and Pb showed a lower content compared to other areas.

It is well-known that metal concentrations in plants vary with plant species (Alloway 1995; Adriano 2013). Table 5 shows that As, Al, Cu, Fe, Co, Cr, Mn, Mo, Sb, Ni, Pb, and Zn content in *Artemisia sieberi* is higher than in *Zygophylum*. These data therefore suggest that the two plants have different capacities for metal uptake. Since *Artemisia sieberi* and

Zygophylum are used as forage, PTEs can be transferred ultimately to animals and humans. Nomads generally spend the spring and summer in settlements in the area, and their cattle and sheep herds graze *Artemisia sieberi* and *Zygophylum* leaves, so they are potentially at risk of PTEs exposure through the food chain.

Bioaccumulation factor (BAF) and translocation factor (TF)—The ability of plants to accumulate metals from contaminated soils was quantified using the BAF (Table 6), which is an indicator of the relative metal bioavailability from soils to plants (Alloway et al. 1988). Plants with BAF_{shoots} values >1 are accumulators, while plants with $BAF_{shoots} < 1$ are excluders (Baker 1981). Additionally, plants are classified as potential hyperaccumulators if the BAF_{shoots} values exceed 10 (Ma et al. 2001).

BAF values vary for each element due to the different solubility of the metal species in soils governing their bioavailability to plants. The ratio is also different between plant species. *Artemisia sieberi* exhibited BAF_{shoots} values < 1 for all elements except for Mn (1.55) and Cd (1.34), indicating that this plant is an accumulator for Mn and Cd. The BAF_{shoots} values for *Artemisia sieberi* were as follows, in decreasing order: Mn > Cd > Cu > Cr > Hg > Sb > Co-Pb > V > Al > As > Fe > Ni > Zn > Mo. The BAF_{shoots} values for *Zygophylum* were <1 for all elements except for Cd (1.65) and were ranked as follows: Cd > Hg > Mo > Cr > Cu-Zn-Sb > Pb> Mn > Ni-V > Fe-Co >AlAs.

BAF_{roots} values for *Artemisia sieberi* were all below 1, suggesting a low efficacy in the phytostabilization of metals in contaminated soils. The order of average BAF_{roots} for *Artemisia sieberi* is Mn > Cd > Pb > Cr > Hg > Co > Cu > Ni > V > As > Al-Fe-Mo-Sb-Zn.

Values in Table 6 for the TF, i.e., the ratio of root to shoot metal content, serve as an indicator of metal transport inside plants, specifically for *Artemisia sieberi* in this study. Plants with TF values >1 are classified as high-efficiency plants for metal trans-location from roots to shoots (Ma et al. 2001). The results revealed that TF exceeded 1 for all metals except Cd, with the following order: Fe > Mo > Mn > Al > Zn > Hg > Sb > Ni > Co > Cu > As > Cr > Pb > V > Cd. The larger TF (>1) for these elements may imply a strong transfer capacity for *Artemisia sieberi*, further supporting that it is a metal accumulator species.

Conclusions

This study characterized PTEs pollution in soils and plants around Gol-E-Gohar mine. The main conclusions are as follows:

i. Elevated concentrations of As, Co, Cu, Fe, and Ni were found in tailings and surface soils around the mine and ore processing plants. Geoaccumulation index values show that some elements such as As, Co, Cu, Fe, and Ni had a $I_{geo} > 1$ in the Tailings and Near areas. The highest recorded concentrations of these elements were in tailing samples. For most elements, concentrations in plant samples decreased with distance away from mining and iron ore processing areas.

ii. Sequential extraction data showed that the major proportion of most studied elements were associated with the residual fraction, reflecting their low bioavailability. Furthermore, MFs for Mn, Zn, Cu, and As indicated that these elements are the most likely to be taken up by plants and living organisms. Chromium, Co, and Fe can be regarded as the most stable PTEs due to their low MFs.

The results of this work have implications for regional air quality and ecosystem health. The soil material is blown in the air and transported in the atmosphere to downwind areas and can affect public health. Also, plant species contaminated with PTEs are used as livestock feed, which may result in PTEs bioaccumulation in living beings feeding on such livestock. Further research is warranted to assess PTE concentrations and distribution in different animal tissues (kidney, hearth, liver, and muscle) and their milk; such results are important in the context of effects on humans after consumption. The region around the GEG mine, and other mines in other regions, require effective measures to reduce toxic metal contamination in soils and plants. For example, practices such as minimizing overgrazing, defining restricted areas for pasture, and grazing in the vicinity of mining sites, and the restoration, rehabilitation, and aftercare of mining sites for pasture and grazing are suggested to reduce PTE levels in livestock.

Supplementary Material

Refer to Web version on PubMed Central for supplementary material.

Acknowledgments

This research was financially supported by Gol-E-Gohar mining and industrial company. The authors also gratefully acknowledge the Shiraz University Research Committee and medical geology research center of Shiraz University for supporting this research. AS acknowledges support from Grant 2 P42 ES04940 from the National Institute of Environmental Health Sciences (NIEHS) Superfund Research Program, NIH, and the Center for Environmentally Sustainable Mining through the TRIF Water Sustainability Program at the University of Arizona. Ahmadreza Khosravi is acknowledged for assistance with plant species identification. Saviz Sehatkashani is acknowledged for the assistance with meteorological data from the Meteorological Organization of Iran.

References

Abreu MM, Santos ES, Ferreira M, Magalhães MCF. *Cistus salviifolius* a promising species for mine wastes remediation. J Geochem Explor. 2012; 113:86–93.

Achiba WB, Lakhdar A, Gabteni N, et al. Accumulation and fractionation of trace metals in a Tunisian calcareous soil amended with farmyard manure and municipal solid waste compost. J Hazard Mater. 2010; 176:99–108. [PubMed: 19945790]

Adriano, DC. Trace elements in the terrestrial environment. Springer Science & Business Media; 2013.

Alavi M. Regional stratigraphy of the Zagros fold-thrust belt of Iran and its proforeland evolution. Am J Sci. 2004; 304:1–20.

Albanese S, De Vivo B, Lima A, Cicchella D. Geochemical background and baseline values of toxic elements in stream sediments of Campania region (Italy). J Geochem Explor. 2007; 93:21–34.

Alloway, BJ. Heavy metals in soils. Springer Science & Business Media; 1995.

Alloway, BJ. Heavy Metals in Soils: Trace Metals and Metalloids in Soils and their Bioavailability, 3, illustr. Springer Science & Business Media; 2012.

Alloway BJ, Thornton I, Smart GA, et al. Metal availability. Sci Total Environ. 1988; 75:41–69. [PubMed: 3222706]

Alvarez E, Marcos MLF, Vaamonde C, Fernández-Sanjurjo MJ. Heavy metals in the dump of an abandoned mine in Galicia (NW Spain) and in the spontaneously occurring vegetation. Sci Total Environ. 2003; 313:185–197. [PubMed: 12922070]

Anjos C, Magalhães MCF, Abreu MM. Metal (Al, Mn, Pb and Zn) soils extractable reagents for available fraction assessment: comparison using plants, and dry and moist soils from the Braçal abandoned lead mine area, Portugal. J Geochem Explor. 2012; 113:45–55.

Anju M, Banerjee DK. Comparison of two sequential extraction procedures for heavy metal partitioning in mine tailings. Chemosphere. 2010; 78:1393–1402. [PubMed: 20106503]

Anju M, Banerjee DK. Associations of cadmium, zinc, and lead in soils from a lead and zinc mining area as studied by single and sequential extractions. Environ Monit Assess. 2011; 176:67–85. [PubMed: 20652631]

Arenas-Lago D, Andrade ML, Lago-Vila M, et al. Sequential extraction of heavy metals in soils from a copper mine: distribution in geochemical fractions. Geoderma. 2014; 230:108–118.

Arenas-Lago D, Andrade ML, Vega FA, Singh BR. TOF-SIMS and FE-SEM/EDS to verify the heavy metal fractionation in serpentinite quarry soils. Catena. 2016; 136:30–43.

Ariza JLG, Giraldez I, Sanchez-Rodas D, Morales E. Metal sequential extraction procedure optimized for heavily polluted and iron oxide rich sediments. Anal Chim Acta. 2000; 414:151–164.

Athar R, Ahmad M. Heavy metal toxicity: effect on plant growth and metal uptake by wheat, and on free living azotobacter. Water Air Soil Pollut. 2002; 138:165–180.

Baker AJM. Accumulators and excluders-strategies in the response of plants to heavy metals. J Plant Nutr. 1981; 3:643–654.

Barnes, HL. Geochemistry of hydrothermal ore deposits. John Wiley & Sons; 1997.

Barton, MD. Iron oxide (−Cu-Au-REE-P-Ag-U-Co) systems. Elsevier Inc; 2013.

Basta NT, McGowen SL. Evaluation of chemical immobilization treatments for reducing heavy metal transport in a smelter-contaminated soil. Environ Pollut. 2004; 127:73–82. [PubMed: 14553997]

Bech J, Corrales I, Tume P, et al. Accumulation of antimony and other potentially toxic elements in plants around a former antimony mine located in the Ribes Valley (Eastern Pyrenees). J Geochem Explor. 2012a; 113:100–105.

Bech J, Duran P, Roca N, et al. Shoot accumulation of several trace elements in native plant species from contaminated soils in the Peruvian Andes. J Geochem Explor. 2012b; 113:106–111.

Benin AL, Sargent JD, Dalton M, Roda S. High concentrations of heavy metals in neighborhoods near ore smelters in northern Mexico. Environ Health Perspect. 1999; 107:279.

Berberian M, King GCP. Towards a paleogeography and tectonic evolution of Iran. Can J Earth Sci. 1981; 18:210–265.

Bes CM, Pardo T, Bernal MP, Clemente R. Assessment of the environmental risks associated with two mine tailing soils from the La Unión-Cartagena (Spain) mining district. J Geochem Explor. 2014; 147:98–106.

Bi X, Feng X, Yang Y, et al. Allocation and source attribution of lead and cadmium in maize (*Zea mays* L.) impacted by smelting emissions. Environ Pollut. 2009; 157:834–839. [PubMed: 19100668]

Bini, C., Bech, J. PHEs, Environment and Human Health: Potentially harmful elements in the environment and the impact on human health. Springer; 2014.

Boularbah A, Schwartz C, Bitton G, et al. Heavy metal contamination from mining sites in South Morocco: 2. Assessment of metal accumulation and toxicity in plants. Chemosphere. 2006; 63:811–817. [PubMed: 16213556]

Cappuyns V, Swennen R, Niclaes M. Application of the BCR sequential extraction scheme to dredged pond sediments contaminated by Pb–Zn mining: a combined geochemical and mineralogical approach. J Geochem Explor. 2007; 93:78–90.

Cerqueira B, Vega FA, Serra C, et al. Time of flight secondary ion mass spectrometry and high-resolution transmission electron microscopy/energy dispersive spectroscopy: a preliminary study of the distribution of Cu 2+ and Cu 2+/Pb 2+ on a Bt horizon surfaces. J Hazard Mater. 2011; 195:422–431. [PubMed: 21920666]

Chai Y, Guo J, Chai S, et al. Source identification of eight heavy metals in grassland soils by multivariate analysis from the Baicheng–Songyuan area, Jilin Province, Northeast China. Chemosphere. 2015; 134:67–75. [PubMed: 25911049]

Chao TT, Zhou L. Extraction techniques for selective dissolution of amorphous iron oxides from soils and sediments. Soil Sci Soc Am J. 1983; 47:225–232.

Chojnacka K, Chojnacki A, Gorecka H, Górecki H. Bioavailability of heavy metals from polluted soils to plants. Sci Total Environ. 2005; 337:175–182. [PubMed: 15626388]

Clemente R, Paredes C, Bernal MP. A field experiment investigating the effects of olive husk and cow manure on heavy metal availability in a contaminated calcareous soil from Murcia (Spain). Agric Ecosyst Environ. 2007; 118:319–326.

Csavina J, Field J, Taylor MP, et al. A review on the importance of metals and metalloids in atmospheric dust and aerosol from mining operations. Sci Total Environ. 2012; 433:58–73. [PubMed: 22766428]

Cui LP, Bai JF, Shi YH, et al. Heavy metals in soil contaminated by coal mining activity. Acta Pedol Sin. 2004; 41:896–904.

Davidson CM, Urquhart GJ, Ajmone-Marsan F, et al. Fractionation of potentially toxic elements in urban soils from five European cities by means of a harmonised sequential extraction procedure. Anal Chim Acta. 2006; 565:63–72.

Delgado J, Barba-Brioso C, Nieto JM, Boski T. Speciation and ecological risk of toxic elements in estuarine sediments affected by multiple anthropogenic contributions (Guadiana saltmarshes, SW Iberian Peninsula): I. Surficial sediments. Sci Total Environ. 2011; 409:3666–3679. [PubMed: 21719073]

Dobran S, Zagury GJ. Arsenic speciation and mobilization in CCA-contaminated soils: influence of organic matter content. Sci Total Environ. 2006; 364:239–250. [PubMed: 16055167]

Dold B. Speciation of the most soluble phases in a sequential extraction procedure adapted for geochemical studies of copper sulfide mine waste. J Geochem Explor. 2003; 80:55–68.

Esmaeili A, Moore F, Keshavarzi B, et al. A geochemical survey of heavy metals in agricultural and background soils of the Isfahan industrial zone, Iran. Catena. 2014; 121:88–98.

Filgueiras AV, Lavilla I, Bendicho C. Chemical sequential extraction for metal partitioning in environmental solid samples. J Environ Monit. 2002a; 4:823–857. [PubMed: 12509036]

Filgueiras A, Lavilla I, Bendicho C. Comparison of the standard SM&T sequential extraction method with small-scale ultrasound-assisted single extractions for metal partitioning in sediments. Anal Bioanal Chem. 2002b; 374:103–108. [PubMed: 12207249]

Frietsch R. On the magmatic origin of iron ores of the Kiruna type. Econ Geol. 1978; 73:478–485.

Galán E, Fernández-Caliani JC, González I, et al. Influence of geological setting on geochemical baselines of trace elements in soils. Application to soils of South–West Spain. J Geochem Explor. 2008; 98:89–106.

García-Ordiales E, Covelli S, Esbrí JM, et al. Sequential extraction procedure as a tool to investigate PTHE geochemistry and potential geoavailability of dam sediments (Almadén mining district, Spain). Catena. 2016; 147:394–403.

Gee GW, Bauder JW, Klute A. Particle-size analysis. Methods soil Anal Part 1 Phys Mineral methods. 1986:383–411.

Gibson MJ, Farmer JG. Multi-step sequential chemical extraction of heavy metals from urban soils. Environ Pollut B. 1986; 11:117–135.

Goldschmidt, VM. The principles of distribution of chemical elements in minerals and rocks. J Chem Soc; The seventh Hugo Müller Lecture, delivered before the Chemical Society; March 17th, 1937; 1937. p. 655-673.

Goldschmidt, VM. Geochemistry. 1958.

Gonnelli, C., Renella, G. Heavy metals in soils. Springer; 2013. Chromium and nickel; p. 313-333.

Guevara-Riba A, Sahuquillo A, Rubio R, Rauret G. Assessment of metal mobility in dredged harbour sediments from Barcelona, Spain. Sci Total Environ. 2004; 321:241–255. [PubMed: 15050399]

Halbach P, Von Borstel D, Gundermann K-D. The uptake of uranium by organic substances in a peat bog environment on a granitic bedrock. Chem Geol. 1980; 29:117–138.

Hall GEM, Gauthier G, Pelchat J-C, et al. Application of a sequential extraction scheme to ten geological certified reference materials for the determination of 20 elements. J Anal At Spectrom. 1996; 11:787–796.

Hauck SA. Petrogenesis and tectonic setting of middle Proterozoic iron oxide–rich ore deposits: an ore deposit model for Olympic Dam-type mineralization. US Geol Surv Bull. 1990; 1932:4–39.

Heydari E. Tectonics versus eustatic control on supersequences of the Zagros Mountains of Iran. Tectonophysics. 2008; 451:56–70.

Hooda, P. Trace elements in soils. John Wiley & Sons; 2010.

Hosseini SA, Asghari O. Multivariate geostatistical simulation of the Gole Gohar iron ore deposit. Iran. 2016; 116:423–430.

Ji K, Kim J, Lee M, et al. Assessment of exposure to heavy metals and health risks among residents near abandoned metal mines in Goseong, Korea. Environ Pollut. 2013; 178:322–328. [PubMed: 23603469]

Kabala C, Singh BR. Fractionation and mobility of copper, lead, and zinc in soil profiles in the vicinity of a copper smelter. J Environ Qual. 2001; 30:485–492. [PubMed: 11285909]

Kabata-Pendias, A. Trace elements in soils and plants. 4. CRC Press; Boca Raton, FL: 2010.

Kahr G, Madsen FT. Determination of the cation exchange capacity and the surface area of bentonite, illite and kaolinite by methylene blue adsorption. Appl Clay Sci. 1995; 9:327–336.

Keshavarzi B, Moore F, Rastmanesh F, Kermani M. Arsenic in the Muteh gold mining district, Isfahan, Iran. Environ Earth Sci. 2012; 67:959–970.

Kisvarsanyi G, Proctor PD. Trace-element content of magnetites and hematites, southeast Missouri metallogenetic province, USA. Econ Geol. 1967; 62:449–471.

Krauskopf KB. Introduction to geochemistry. International series in the earth and planetary sciences. 1979

Kříbek B, Majer V, Pašava J, et al. Contamination of soils with dust fallout from the tailings dam at the Rosh Pinah area, Namibia: regional assessment, dust dispersion modeling and environmental consequences. J Geochem Explor. 2014; 144:391–408.

Levei E, Frentiu T, Ponta M, et al. Characterization and assessment of potential environmental risk of tailings stored in seven impoundments in the Aries river basin, Western Romania. Chem Cent J. 2013; 7:5. [PubMed: 23311708]

Levinson, AA. Introduction to exploration geochemistry. [Textbook]. 1974.

Li X, Coles BJ, Ramsey MH, Thornton I. Chemical partitioning of the new National Institute of Standards and Technology standard reference materials (SRM 2709–2711) by sequential extraction using inductively coupled plasma atomic emission spectrometry. Analyst. 1995; 120:1415–1419.

Li Y, Wang H, Wang H, et al. Heavy metal pollution in vegetables grown in the vicinity of a multi-metal mining area in Gejiu, China: total concentrations, speciation analysis, and health risk. Environ Sci Pollut Res. 2014; 21:12569–12582.

Li P, Lin C, Cheng H, et al. Contamination and health risks of soil heavy metals around a lead/zinc smelter in southwestern China. Ecotoxicol Environ Saf. 2015; 113:391–399. [PubMed: 25540851]

Liénard A, Brostaux Y, Colinet G. Soil contamination near a former Zn–Pb ore-treatment plant: Evaluation of deterministic factors and spatial structures at the landscape scale. J Geochem Explor. 2014; 147:107–116.

Liu Z, Pan S, Sun Z, et al. Heavy metal spatial variability and historical changes in the Yangtze River estuary and North Jiangsu tidal flat. Mar Pollut Bull. 2015; 98:115–129. [PubMed: 26159727]

Liu G, Wang J, Zhang E, et al. Heavy metal speciation and risk assessment in dry land and paddy soils near mining areas at Southern China. Environ Sci Pollut Res. 2016; 23:8709–8720.

Loska K, Wiechula D, Korus I. Metal contamination of farming soils affected by industry. Environ Int. 2004; 30:159–165. [PubMed: 14749104]

Luo L, Chu B, Liu Y, et al. Distribution, origin, and transformation of metal and metalloid pollution in vegetable fields, irrigation water, and aerosols near a Pb-Zn mine. Environ Sci Pollut Res. 2014; 21:8242–8260.

Ma LQ, Komart KM, Tu C, et al. A Fern that Hyperaccumulates Arsenic A hardy, versatile, fast-growing plant helps to remove arsenic from contaminated soils [J]. World Environ. 2001; 3:47–48.

Ma L, Yang Z, Li L, Wang L. Source identification and risk assessment of heavy metal contaminations in urban soils of Changsha, a mine-impacted city in Southern China. Environ Sci Pollut Res. 2016:1–9.

Maiz I, Esnaola MV, Millan E. Evaluation of heavy metal availability in contaminated soils by a short sequential extraction procedure. Sci Total Environ. 1997; 206:107–115.

Mazdab FK. The distribution of trace elements in iron sulfides and associated chlorine-bearing silicates. 2001

Meunier, A. Clays. Springer Science & Business Media; New York: 2005.

Monjezi M, Rezaei M, Varjani AY. Prediction of rock fragmentation due to blasting in Gol-E-Gohar iron mine using fuzzy logic. Int J Rock Mech Min Sci. 2009; 46:1273–1280.

Monteiro LVS, Xavier RP, Hitzman MW, et al. Mineral chemistry of ore and hydrothermal alteration at the Sossego iron oxide–copper–gold deposit, Carajás Mineral Province, Brazil. Ore Geol Rev. 2008; 34:317–336.

Monterroso C, Rodríguez F, Chaves R, et al. Heavy metal distribution in mine-soils and plants growing in a Pb/Zn-mining area in NW Spain. Appl Geochem. 2014; 44:3–11.

Moore, DM., Reynolds, RC. X-ray diffraction and the identification and analysis of clay minerals. Oxford university press; Oxford: 1997.

Moore F, Dehbandi R, Keshavarzi B, Amjadian K. Potentially toxic elements in the soil and two indigenous plant species in Dashkasan epithermal gold mining area, West Iran. Environ Earth Sci. 2016; 75:1–16.

Moreno-Jiménez E, Peñalosa JM, Manzano R, et al. Heavy metals distribution in soils surrounding an abandoned mine in NW Madrid (Spain) and their transference to wild flora. J Hazard Mater. 2009; 162:854–859. [PubMed: 18603359]

Mücke, A., Golestaneh, F. The genesis of the Gol Gohar iron ore deposit (Iran). Institu fur Mineral und Kritallographieder Tech Univ; Berlin: 1982. p. 193-212.

Mücke A, Younessi R. Magnetite-apatite deposits (Kiruna-type) along the Sanandaj-Sirjan zone and in the Bafq area, Iran, associated with ultramafic and calcalkaline rocks and carbonatites. Mineral Petrol. 1994; 50:219–244.

Müller G. Index of geoaccumulation in sediments of the Rhine River. Geol J. 1969; 2:108–118.

Nabatian G, Rastad E, Neubauer F, et al. Iron and Fe–Mn mineralisation in Iran: implications for Tethyan metallogeny. Aust J Earth Sci. 2015; 62:211–241.

Nelson DW, Sommers LE, Sparks DL, et al. Total carbon, organic carbon, and organic matter. Methods soil Anal Part 3-chemical methods. 1996:961–1010.

Nemati K, Bakar NKA, Abas MR. Investigation of heavy metals mobility in shrimp aquaculture sludge—comparison of two sequential extraction procedures. Microchem J. 2009; 91:227–231.

Nyamangara J. Use of sequential extraction to evaluate zinc and copper in a soil amended with sewage sludge and inorganic metal salts. Agric Ecosyst Environ. 1998; 69:135–141.

Osakwe SA. Chemical partitioning of iron, cadmium, nickel and chromium in contaminated soils of south-eastern Nigeria. Chem Speciat Bioavailab. 2013; 25:71–78.

Pal DC, Barton MD, Sarangi AK. Deciphering a multistage history affecting U–Cu (−Fe) mineralization in the Singhbhum Shear Zone, eastern India, using pyrite textures and compositions in the Turamdih U–Cu (−Fe) deposit. Miner Depos. 2009; 44:61–80.

Pascual JA, Garcia C, Hernandez T, Ayuso M. Changes in the microbial activity of an arid soil amended with urban organic wastes. Biol Fertil Soils. 1997; 24:429–434.

Pirajno, F. Hydrothermal Processes and Mineral Systems. Springer; 2009. Hydrothermal processes associated with meteorite impacts; p. 1097-1130.

Prabhakar G, Sorooshian A, Toffol E, et al. Spatiotemporal distribution of airborne particulate metals and metalloids in a populated arid region. Atmos Environ. 2014; 92:339–347.

Pueyo M, Mateu J, Rigol A, et al. Use of the modified BCR three-step sequential extraction procedure for the study of trace element dynamics in contaminated soils. Environ Pollut. 2008; 152:330–341. [PubMed: 17655986]

Qiao Y, Yang Y, Gu J, Zhao J. Distribution and geochemical speciation of heavy metals in sediments from coastal area suffered rapid urbanization, a case study of Shantou Bay, China. Mar Pollut Bull. 2013; 68:140–146. [PubMed: 23290610]

Qin F, Ji H, Li Q, et al. Evaluation of trace elements and identification of pollution sources in particle size fractions of soil from iron ore areas along the Chao River. J Geochem Explor. 2014; 138:33–49.

Ramos-Miras JJ, Roca-Perez L, Guzmán-Palomino M, et al. Background levels and baseline values of available heavy metals in Mediterranean greenhouse soils (Spain). J Geochem Explor. 2011; 110:186–192.

Rashed MN. Monitoring of contaminated toxic and heavy metals, from mine tailings through age accumulation, in soil and some wild plants at Southeast Egypt. J Hazard Mater. 2010; 178:739–746. [PubMed: 20188467]

Rastegari Mehr M, Keshavarzi B, Moore F, et al. Contamination level and human health hazard assessment of heavy metals and polycyclic aromatic hydrocarbons (PAHs) in street dust deposited in Mahshahr, southwest of Iran. Hum Ecol Risk Assess Int J. 2016; 22:1726–1748.

Rastmanesh F, Moore F, Keshavarzi B. Speciation and phytoavailability of heavy metals in contaminated soils in Sarcheshmeh area, Kerman Province, Iran. Bull Environ Contam Toxicol. 2010; 85:515–519. [PubMed: 21069278]

Rattan RK, Datta SP, Chhonkar PK, et al. Long-term impact of irrigation with sewage effluents on heavy metal content in soils, crops and groundwater—a case study. Agric Ecosyst Environ. 2005; 109:310–322.

Rauret G. Extraction procedures for the determination of heavy metals in contaminated soil and sediment. Talanta. 1998; 46:449–455. [PubMed: 18967165]

Reimann C, Filzmoser P. Normal and lognormal data distribution in geochemistry: death of a myth. Consequences for the statistical treatment of geochemical and environmental data. Environ Geol. 2000; 39:1001–1014.

Reimann C, Filzmoser P, Garrett RG. Background and threshold: critical comparison of methods of determination. Sci Total Environ. 2005; 346:1–16. [PubMed: 15993678]

Rodríguez L, Ruiz E, Alonso-Azcárate J, Rincón J. Heavy metal distribution and chemical speciation in tailings and soils around a Pb–Zn mine in Spain. J Environ Manag. 2009; 90:1106–1116.

Rose, AW., Hawkes, HE., Webb, JS. Geochemistry in mineral exploration. Academic Pr; 1979.

Rusk B, Oliver N, Cleverley J, et al. Physical and chemical characteristics of the Ernest Henry iron oxide copper gold deposit, Australia; implications for IOGC genesis. 2010

Ryser P, Sauder WR. Effects of heavy-metal-contaminated soil on growth, phenology and biomass turnover of *Hieracium piloselloides*. Environ Pollut. 2006; 140:52–61. [PubMed: 16185797]

Salminen R, Tarvainen T. The problem of defining geochemical baselines. A case study of selected elements and geological materials in Finland. J Geochem Explor. 1997; 60:91–98.

Shafie NA, Aris AZ, Zakaria MP, et al. Application of geoaccumulation index and enrichment factors on the assessment of heavy metal pollution in the sediments. J Environ Sci Healh A. 2013; 48:182–190.

Sheikholeslami MR, Pique A, Mobayen P, et al. Tectono-metamorphic evolution of the Neyriz metamorphic complex, Qurikor-e-sefid area (Sanandaj-Sirjan Zone, SW Iran). J Asian Earth Sci. 2008; 31:504–521.

Siegel, FR. Environmental geochemistry of potentially toxic metals. Springer; New York: 2002.

Sipos P, Choi C, May Z. Combination of single and sequential chemical extractions to study the mobility and host phases of potentially toxic elements in airborne particulate matter. Chemie Erde-Geochem. 2016; 76:481–489.

Slack, JF., Johnson, CA., Lund, KI., et al. A new model for Co-Cu-Au deposits in metasedimentary rocks—an IOCG connection?. Proceedings of the 11th Biennial SGA Meeting; Antofagasta, Chile. 2011. p. 489-491.

Soltani N, Moore F, Keshavarzi B, Sharifi R. Geochemistry of trace metals and rare earth elements in stream water, stream sediments and acid mine drainage from darrehzar copper mine, Kerman, Iran. Water Qual Expo Health. 2014; 6:97–114.

Soltani N, Keshavarzi B, Sorooshian A, et al. Oxidative potential (OP) and mineralogy of iron ore particulate matter at the Gol-E-Gohar Mining and Industrial Facility (Iran). Environ Geochem Health. 2017; doi: 10.1007/s10653-017-9926-5

Sorooshian A, Csavina J, Shingler T, et al. Hygroscopic and chemical properties of aerosols collected near a copper smelter: implications for public and environmental health. Environ Sci Technol. 2012; 46:9473–9480. [PubMed: 22852879]

Sposito G. The chemical forms of trace metals in soils. Appl Environ Geochem. 1983:123–170.

Stevenson FJ. Trace metal-organic matter interactions in geologic environments. 1983

Stocklin J. Structural history and tectonics of Iran: a review. Am Assoc Pet Geol Bull. 1968; 52:1229–1258.

Stone M, Droppo IG. Distribution of lead, copper and zinc in size-fractionated river bed sediment in two agricultural catchments of southern Ontario, Canada. Environ Pollut. 1996; 93:353–362. [PubMed: 15093532]

Sun Y, Zhou Q, Diao C. Effects of cadmium and arsenic on growth and metal accumulation of Cd-hyperaccumulator *Solanum nigrum* L. Bioresour Technol. 2008; 99:1103–1110. [PubMed: 17719774]

Sun Y, Zhou Q, Wang L, Liu W. Cadmium tolerance and accumulation characteristics of *Bidens pilosa* L. as a potential Cd-hyperaccumulator. J Hazard Mater. 2009; 161:808–814. [PubMed: 18513866]

Taylor MP, Mackay AK, Hudson-Edwards KA, Holz E. Soil Cd, Cu, Pb and Zn contaminants around Mount Isa city, Queensland, Australia: potential sources and risks to human health. Appl Geochem. 2010; 25:841–855.

Teng Y, Ni S, Wang J, et al. A geochemical survey of trace elements in agricultural and non-agricultural topsoil in Dexing area, China. J Geochem Explor. 2010; 104:118–127.

Tessier A, Campbell PGC, Bisson M. Sequential extraction procedure for the speciation of particulate trace metals. Anal Chem. 1979; 51:844–851.

Thanabalasingam P, Pickering WF. The sorption of mercury (II) by humic acids. Environ Pollut B. 1985; 9:267–279.

Tume P, Bech J, Tume L, et al. Concentrations and distributions of Ba, Cr, Sr, V, Al, and Fe in Torrelles soil profiles (Catalonia, Spain). J Geochem Explor. 2008; 96:94–105.

Uren NC. Forms, reactions, and availability of nickel in soils. Adv Agron. 1992; 48:141–203.

Vega FA, Andrade ML, Covelo EF. Influence of soil properties on the sorption and retention of cadmium, copper and lead, separately and together, by 20 soil horizons: comparison of linear regression and tree regression analyses. J Hazard Mater. 2010; 174:522–533. [PubMed: 19811872]

Vithanage M, Rajapaksha AU, Oze C, et al. Metal release from serpentine soils in Sri Lanka. Environ Monit Assess. 2014; 186:3415–3429. [PubMed: 24464398]

Williams PJ, Barton MD, Johnson DA, et al. Iron oxide copper-gold deposits: geology, space-time distribution, and possible modes of origin. Econ Geol. 2005:371–405.

Xavier RP, Monteiro LVS, Moreto CPN, et al. The iron oxide copper-gold systems of the Carajás mineral province, Brazil. Soc Econ Geol. 2012:433–454.

Yan C, Li Q, Zhang X, Li G. Mobility and ecological risk assessment of heavy metals in surface sediments of Xiamen Bay and its adjacent areas, China. Environ Earth Sci. 2010; 60:1469–1479.

Yoon J, Cao X, Zhou Q, Ma LQ. Accumulation of Pb, Cu, and Zn in native plants growing on a contaminated Florida site. Sci Total Environ. 2006; 368:456–464. [PubMed: 16600337]

Zhu N, Qiang L, Guo X, et al. Sequential extraction of anaerobic digestate sludge for the determination of partitioning of heavy metals. Ecotoxicol Environ Saf. 2014; 102:18–24. [PubMed: 24580817]

Zumdahl, S., DeCoste, DJ. Cengage Learning. 8. 2014. Introductory chemistry: A foundation.

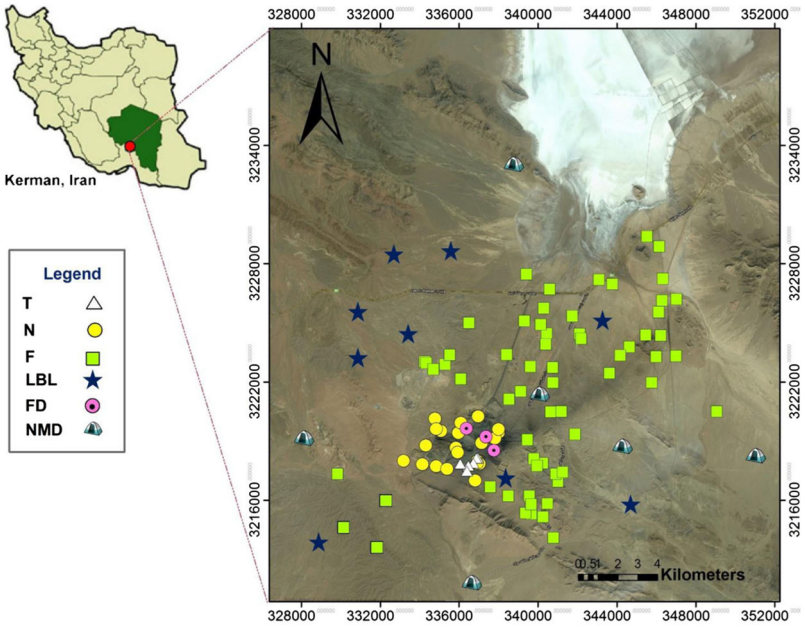

Fig. 1.

Map showing the study site location at Gol-E-Gohar iron ore mine. *Yellow, white, green, and dark blue markers* in the right image represent the locations where soil (N, F, LBL) and tailing (T) samples were collected. *Purple markers* indicate where fallout dust (FD) samples were collected. *T* tailings, *N* near, *F* far, *LBL* local baseline, *FD* fallout dust, *NMD* nomads

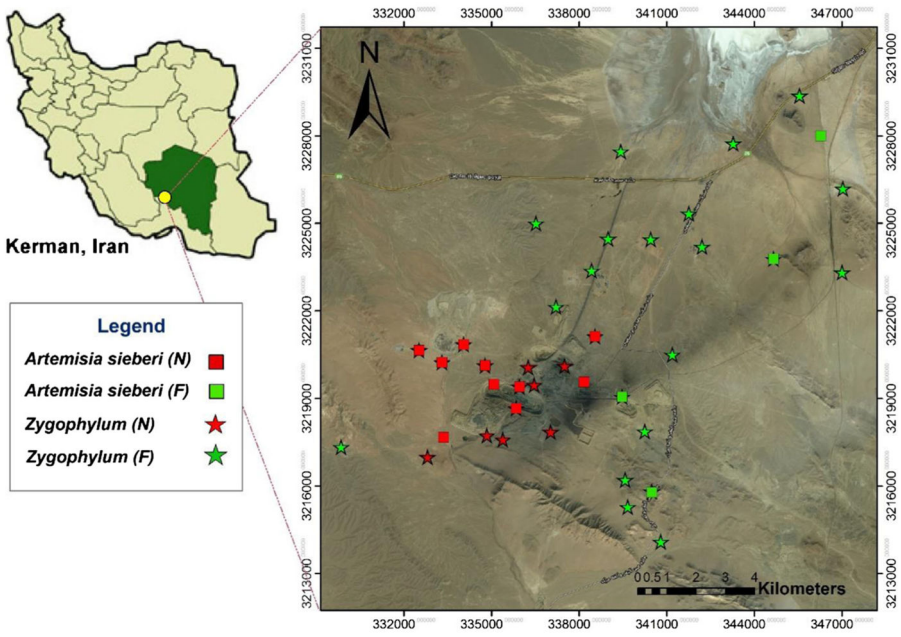

Fig. 2.

Plant sampling locations for *Artemisia sieberi* and *Zygophylum* species in the Near and Far areas of the mine and processing plants

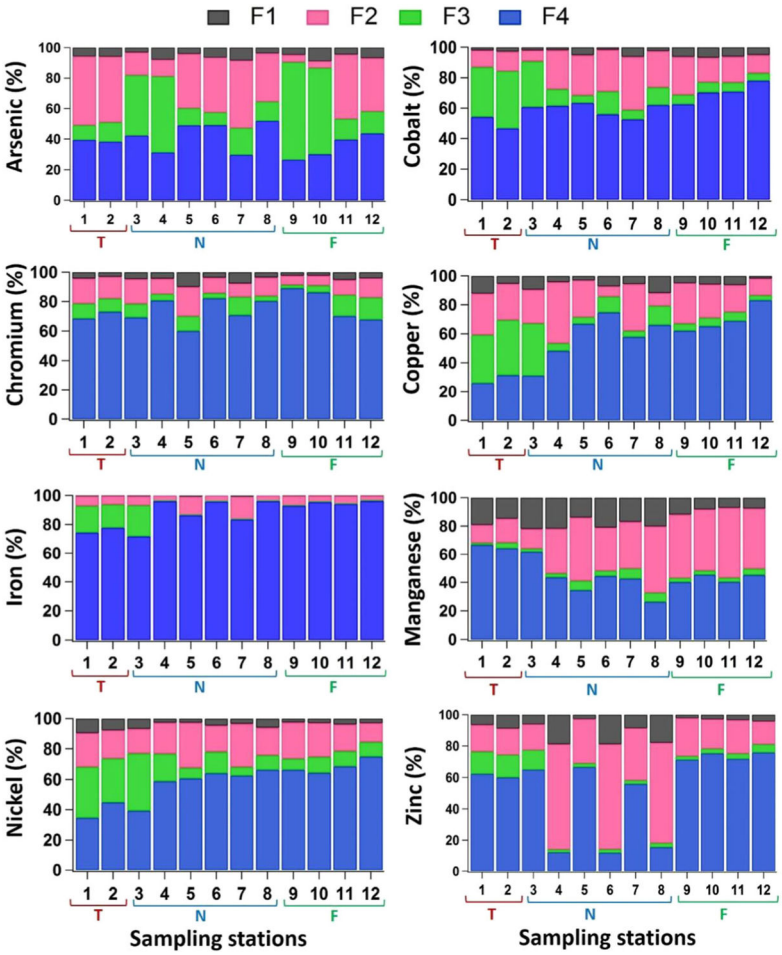

Fig. 3.

Percentage of As, Co, Cr, Cu, Fe, Mn, Ni, and Zn extracted in each step of the sequential extraction procedure. Fraction 1: exchangeable and associated with carbonates; Fraction 2: associated with easily and moderately reducible iron and manganese oxyhydroxides; Fraction 3: associated with SOM and sulfides; Fraction 4: aqua-regia extractable residual fraction. Locations: 1 and 2 in Tailings (T); 3, 4, 5, 6, 7, and 8 in Near area of the mine (N); 9, 10, 11, and 12 in Far area of the mine (F)

Table 1

Physicochemical properties of “Tailings” and soil samples at GEG mine divided into the three categories representing where the samples were collected relative to activities associated with iron ore mining and mineral processing (Near, Far, Tailing). Percentages below are on a mass basis

Area		OM %	pH	EC (μs cm^{-1})	CEC (meq 100 g^{-1})	Silt %	Clay %	Sand %
Near (*N* = 13)	Mean	0.55	7.79	1825.59	9.24	24.85	16.43	58.72
	Median	0.28	7.97	486.20	8.40	24.36	17.48	57.80
	Min	0.07	6.87	260.90	1.80	8.36	7.48	46.52
	Max	1.52	8.63	8903.00	20.00	36.00	19.48	84.16
Far (*N* = 25)	Mean	0.60	7.90	1988.92	8.16	26.12	18.03	55.86
	Median	0.55	7.97	481.40	8.30	24.64	17.20	58.52
	Min	0.07	6.88	235.10	1.80	14.64	14.20	18.52
	Max	1.31	8.26	8754.00	11.00	62.92	34.56	68.52
Tailings (*N* = 1)	Mean	0.24	7.28	2599.00	6.80	9.64	10.20	80.16
Cumulative (*N* = 39)	Mean	0.57	7.85	1746.84	8.49	25.27	17.29	57.43

Based on cumulative data at the study site, the soil exhibited a clayey loam texture (i.e., 25.27% silt, 17.29% clay, and 57.43% sand).

Table 2

Statistical analysis of PTE concentrations in Tailings and soil samples at GEG mine (total concentrations in mg kg^{-1} except for Hg in μg kg^{-1}) as determined by ICP-MS. *MDL* method detection limit, *SD* standard deviation, *CV SD/mean* coefficient of variation, I_{geo} geoaccumulation index, *NA* not analyzed

	Al	As	Cd	Co	Cr	Cu	Fe	Hg	Mn	Mo	Ni	Pb	Sb	V	Zn
MDL	100	0.1	0.02	0.1	0.5	0.01	100	5	1	0.01	0.1	0.01	0.02	2	0.1
Mean Tailings, (N=7)	13114.29	25.39	0.05	189.83	26.03	472.77	120642.86	24.86	318.57	2.20	150.29	2.64	0.16	62.57	44.53
Median	12800.00	28.40	0.05	187.20	26.00	406.01	116200.00	30.00	318.00	2.13	124.80	2.42	0.16	66.00	38.90
Min	12200.00	14.40	0.02	130.90	20.40	330.98	98100.00	<MDL	245.00	1.62	118.50	2.08	0.13	42.00	35.80
Max	14800.00	33.00	0.12	261.50	32.60	885.03	168200.00	37.00	374.00	2.63	278.10	3.65	0.20	77.00	77.70
SD	911.83	7.48	0.03	43.66	3.98	186.42	23190.15	0.79	42.77	0.38	58.36	0.54	0.03	13.56	14.87
VC	0.07	0.29	0.59	0.23	0.15	0.39	0.19	0.32	0.13	0.17	0.39	0.20	0.16	0.22	0.33
Igeo	−1.19	0.67	−2.80	3.02	−1.75	3.10	1.49	−1.78	−1.72	1.30	0.45	−3.04	−1.19	−0.38	−1.34
Mean Near, (N= 29)	20685.19	16.00	0.16	38.50	48.07	100.84	101588.89	22.30	544.63	1.02	74.69	10.80	0.22	92.33	72.96
Median	19200.00	13.90	0.17	21.60	45.40	53.85	61200.00	26.00	538.00	0.87	73.20	11.29	0.13	79.00	64.70
Min	4200.00	9.20	0.02	11.80	14.60	17.36	21700.00	<MDL	189.00	0.40	28.10	2.25	0.06	33.00	28.10
Max	57100.00	35.80	0.33	137.00	126.00	386.63	400000.00	47.00	716.00	2.93	132.60	17.42	0.71	203.00	350.90
SD	10458.44	6.59	0.08	33.76	21.61	98.35	93420.65	13.82	134.00	0.55	22.78	4.15	0.17	46.28	56.97
VC	0.51	0.41	0.48	0.88	0.45	0.98	0.92	0.62	0.25	0.54	0.30	0.38	0.80	0.50	0.78
Igeo	−0.68	0.04	−1.31	0.36	−0.99	0.43	0.62	−1.56	−4.31	0.04	−0.56	−1.15	−1.07	0.04	−0.74
Mean Far, (N= 64)	20253.13	11.77	0.22	16.51	53.21	38.95	33428.13	31.45	643.84	0.73	71.56	15.07	0.21	55.38	71.91
Median	18950.00	11.55	0.21	15.75	52.65	35.99	31100.00	30.50	649.00	0.65	71.50	13.53	0.20	53.00	69.00
Min	10500.00	7.40	0.09	7.90	28.10	17.17	12500.00	4.00	378.00	0.40	36.00	5.95	0.08	29.00	35.90
Max	59400.00	19.40	0.61	30.90	104.00	83.53	72600.00	57.00	797.00	1.59	86.70	64.68	0.87	107.00	180.70
SD	6668.55	1.99	0.07	3.68	9.31	11.04	9188.70	11.11	76.13	0.26	7.94	8.28	0.12	11.64	18.69
VC	0.33	0.17	0.33	0.22	0.17	0.28	0.27	0.35	0.12	0.36	0.11	0.55	0.60	0.21	0.26
Igeo	−0.61	−0.40	−0.62	−0.51	−0.72	−0.48	−0.39	−1.35	−0.70	−0.34	−0.56	−0.61	−0.98	−0.55	−0.63
Local baseline (N=9)	19900.00	10.20	0.22	15.30	57.80	35.01	28200.00	49.00	693.00	0.59	70.10	14.29	0.24	53.00	72.40
World soil average[a]	71000.00	4.70	1.10	6.90	42.00	14.00	35000.00	100.00	418.00	1.18	18.00	25.00	0.48	60.00	62.00
Fallout dust (N=10)	15736.29	12.63	0.04	104.10	30.43	270.45	326363.67	NA	269.98	1.78	98.65	2.53	0.22	166.89	44.83

[a]Kabata-Pendias (2010)

Table 3

Correlation coefficient (*r* value) between PTE concentrations in “Tailings” and soil samples (*N* = 100). *significant at 95% based on two-tailed student’s *t* test, **significant at 99%

	Al	As	Cd	Co	Cr	Cu	Fe	Hg	Mn	Mo	Ni	Pb	Sb	V	Zn
Al	1														
As	−0.175	1													
Cd	0.357**	−0.191	1												
Co	0.004	0.557**	−.376**	1											
Cr	0.810**	−0.321**	0.413**	−0.16	1										
Cu	−0.075	0.630**	−0.167	0.871**	−0.299**	1									
Fe	0.001	0.598**	−0.310**	0.955**	−0.205*	0.904**	1								
Hg	0.023	−0.085	0.154	−0.078	0.068	0.019	−0.021	1							
Mn	0.498**	0.219*	0.648**	−0.383**	0.613**	−0.312**	−0.347**	0.188	1						
Mo	−0.019	0.349**	−0.118	0.641**	−0.173	0.723**	0.656**	0.077	−0.304**	1					
Ni	0.196	0.316**	−0.043	0.509**	0.303**	0.446**	0.423**	0.024	0.098	0.452**	1				
Pb	0.271**	−0.202	0.738**	−0.378**	0.432**	−0.213*	−0.294**	0.284**	0.626**	−0.162	−0.091	1			
Sb	0.029	0.115	0.521**	−0.092	0.009	0.126	0.036	0.256*	0.147	0.201*	0.039	0.463**	1		
V	0.236*	0.425**	−0.182	0.742**	0.099	0.680**	0.760**	0.008	−0.250*	0.534**	0.395**	−0.206*	−0.005	1	
Zn	0.439**	−0.174	0.630**	−0.165	0.492**	−0.052	−0.121	0.123	0.561**	0.052	0.08	0.711**	0.301**	−0.037	1

Environ Sci Pollut Res Int. Author manuscript; available in PMC 2017 December 01.

Table 4

Matrix of PCA loadings in “Tailings” and soil samples from GEG mine

	Component			
Element	**1**	**2**	**3**	**Communities**
Al	−0.02	*0.943*	0.014	0.891
As	*0.709*	−0.127	−0.072	0.525
Cd	−0.411	0.403	*0.659*	0.766
Co	*0.854*	−0.132	−0.346	0.866
Cr	−0.39	*0.859*	0.074	0.895
Cu	*0.853*	−0.122	−0.346	0.861
Fe	*0.895*	−0.067	0.026	0.806
Hg	−0.114	0.117	0.231	0.099
Mn	0.449	*0.667*	0.221	0.765
Mo	*0.865*	0.038	−0.24	0.807
Ni	*0.678*	0.107	−0.367	0.605
Pb	−0.285	0.195	0.773	0.717
Sb	0.284	*0.506*	0.281	0.684
V	*0.627*	0.066	0.147	0.42
Zn	0.111	0.021	*0.793*	0.642
Initial Eigenvalue	6.421	2.495	1.434	
Total variance %	42.807	16.634	9.561	
Cumulative %	42.807	59.441	69.002	

Italic values represent higher factor loadings

Table 5

Statistical analysis of PTE concentrations (mg kg^{-1}) in shoots and roots of two abundant plant species (*Artemisia sieberi* and *Zygophylum*) in Near and Far areas of GEG area

	Artemisia sieberi								**Zygophylum**			
	Shoots (N=36)				**Roots (N=10)**				**(N=14)**			
	Near (N=14)		**Far (N=22)**		**Near (N=5)**		**Far (N=5)**		**Near (N=9)**		**Far (N=5)**	
	Mean	**Range**	**Mean**	**Range**	**Mean**	**Range**	**Mean**	**Range**	**Mean**	**Range**	**Mean/SD**	**Range**
Al	1135.71	500.00–1900.00	1012.73	80.00–2300.00	540.00	300.00–900.00	640.00	500.00–900.00	122.22	100.00–200.00	88.00	80.00–100.00
As	1.54	0.50–2.50	1.12	0.08–2.00	0.64	0.20–1.20	0.48	0.30–0.80	0.17	0.10–0.50	0.12	0.08–0.30
Cd	0.06	0.03–0.11	0.11	0.04–1.25	0.36	0.05–1.52	0.07	0.05–0.09	0.27	0.07–0.48	0.17	0.06–0.26
Co	2.79	0.66–6.02	1.28	0.42–2.63	1.22	0.70–1.66	0.61	0.48–0.77	0.58	0.31–0.81	0.36	0.28–0.41
Cr	7.39	3.70–16.40	5.57	1.20–8.20	5.32	4.10–7.60	6.14	5.00–7.90	2.00	1.70–2.20	1.62	1.30–1.80
Cu	31.70	14.62–51.52	17.8	1.72–26.45	15.15	13.17–17.28	11.31	8.80–12.56	9.62	6.41–14.40	4.33	2.31–8.89
Fe	6764.29	1360.00–18450.00	3229.09	770.00–6520.00	1974.00	1860.00–2370.00	1106.00	980.00–1290.00	1111.11	580.00–2210.00	592.00	460.00–730.00
Hg	0.04	0.02–0.08	0.03	0.02–0.06	0.02	0.01–0.04	0.02	0.01–0.03	0.03	0.02–0.04	0.02	0.02–0.03
Mn	93.79	65.00–132.00	84.82	27.00–125.00	40.40	31.00–61.00	39.20	34.00–45.00	59.56	47.00–82.00	38.00	26.00–56.00
Mo	1.08	0.55–2.30	0.87	0.31–3.36	0.53	0.36–0.82	0.37	0.16–0.56	0.62	0.18–2.30	0.35	0.12–0.62
Ni	7.45	3.60–10.90	5.59	0.30–9.50	3.30	2.30–4.70	3.30	2.40–4.50	2.86	2.00–3.70	2.36	1.80–3.20
Pb	1.24	0.65–3.13	1.61	0.16–4.12	0.50	0.27–0.84	0.55	0.43–0.78	0.15	0.10–0.19	0.23	0.12–0.33
Sb	0.07	0.05–0.16	0.09	0.02–0.16	0.04	0.02–0.05	0.04	0.03–0.05	0.02	0.02–0.03	0.03	0.02–0.03
V	2.04	1.50–3.00	2.91	1.50–7.00	1.70	1.50–2.00	1.80	1.50–2.00	2.00	2.00–2.00	1.60	1.50–1.80
Zn	64.95	13.80–397.40	21.80	2.60–42.00	39.86	10.30–148.30	10.02	7.90–12.80	15.19	4.50–61.50	6.90	2.30–18.10

Table 6

Bioaccumulation factor (BAF) and translocation factor (TF) for PTEs in shoots and roots of *Artemisia sieberi* and shoots of *Zygophylum* of GEG area

	Artemisia sieberi			***Zygophylum***
	TF	**BAF_{shoots}**	**BAF_{roots}**	**BAF_{shoots}**
Al	2.33	0.19	0.03	0.01
As	1.43	0.17	0.04	0.01
Cd	0.88	1.34	0.55	1.65
Co	2.05	0.57	0.20	0.03
Cr	1.15	0.66	0.26	0.29
Cu	1.87	0.70	0.09	0.23
Fe	3.14	0.15	0.03	0.03
Hg	2.20	0.59	0.21	0.94
Mn	2.42	1.55	0.78	0.09
Mo	2.49	0.06	0.03	0.78
Ni	2.13	0.13	0.08	0.04
Pb	1.12	0.57	0.49	0.18
Sb	2.16	0.58	0.03	0.23
V	1.00	0.49	0.05	0.04
Zn	2.23	0.11	0.03	0.23